LETTERS

New role of bone morphogenetic protein 7 in brown adipogenesis and energy expenditure

Yu-Hua Tseng[1], Efi Kokkotou[3], Tim J. Schulz[1], Tian Lian Huang[1], Jonathon N. Winnay[1], Cullen M. Taniguchi[1], Thien T. Tran[1], Ryo Suzuki[1], Daniel O. Espinoza[1], Yuji Yamamoto[1], Molly J. Ahrens[4], Andrew T. Dudley[4], Andrew W. Norris[5], Rohit N. Kulkarni[2] & C. Ronald Kahn[1]

Adipose tissue is central to the regulation of energy balance. Two functionally different types of fat are present in mammals: white adipose tissue, the primary site of triglyceride storage, and brown adipose tissue, which is specialized in energy expenditure and can counteract obesity[1]. Factors that specify the developmental fate and function of white and brown adipose tissue remain poorly understood[2,3]. Here we demonstrate that whereas some members of the family of bone morphogenetic proteins (BMPs) support white adipocyte differentiation, BMP7 singularly promotes differentiation of brown preadipocytes even in the absence of the normally required hormonal induction cocktail. BMP7 activates a full program of brown adipogenesis including induction of early regulators of brown fat fate PRDM16 (PR-domain-containing 16; ref. 4) and PGC-1α (peroxisome proliferator-activated receptor-γ (PPARγ) coactivator-1α; ref. 5), increased expression of the brown-fat-defining marker uncoupling protein 1 (UCP1) and adipogenic transcription factors PPARγ and CCAAT/enhancer-binding proteins (C/EBPs), and induction of mitochondrial biogenesis via p38 mitogen-activated protein (MAP) kinase-(also known as Mapk14) and PGC-1-dependent pathways. Moreover, BMP7 triggers commitment of mesenchymal progenitor cells to a brown adipocyte lineage, and implantation of these cells into nude mice results in development of adipose tissue containing mostly brown adipocytes. *Bmp7* knockout embryos show a marked paucity of brown fat and an almost complete absence of UCP1. Adenoviral-mediated expression of BMP7 in mice results in a significant increase in brown, but not white, fat mass and leads to an increase in energy expenditure and a reduction in weight gain. These data reveal an important role of BMP7 in promoting brown adipocyte differentiation and thermogenesis *in vivo* and *in vitro*, and provide a potential new therapeutic approach for the treatment of obesity.

BMPs are members of the transforming growth factor-β (TGF-β) superfamily and control multiple key steps of embryonic development and differentiation[6]. BMPs seem to have different roles in adipogenesis[7]. Although certain BMPs, in particular BMP2 and BMP4, enhance white adipogenesis when assisted by a hormonal induction cocktail[8,9], the role of BMPs in the differentiation and function of brown adipose tissue (BAT) or the balance between white adipose tissue (WAT) and BAT is unknown. To this end, we studied the role of BMPs in the differentiation of brown preadipocytes[10] and 3T3-L1 white preadipocytes in the absence of other hormonal or chemical inducers. Treatment of these cells with BMP2, BMP4, BMP6 and BMP7 markedly increased lipid accumulation of brown preadipocytes in culture even in the absence of the normally required induction cocktail or thiazolidinediones (Fig. 1a). BMP5 exhibited a weaker effect compared to other BMPs, and BMP3 had virtually no effect on brown fat differentiation. In contrast, under the same conditions, 3T3-L1 white preadipocytes exhibited little or no differentiation when treated with these BMPs.

In brown preadipocytes, whereas BMP2, BMP4, BMP6 and BMP7 induced lipid accumulation to similar extents, BMP7 was unique in that it markedly induced *Ucp1* messenger RNA expression (Fig. 1b) to a level comparable to that achieved by standard induction protocols (Supplementary Table 1). In addition, expression of several other brown-fat-selective genes was significantly induced by BMP7 (Supplementary Fig. 1). In contrast, BMP4, an adipogenic factor for white fat[9], suppressed expression of *Ucp1* in these brown preadipocytes (Fig. 1b), despite its effect on lipid accumulation (Fig. 1a). Western blot analysis confirmed the specific effect of BMP7 on induction of UCP1 protein expression in brown, but not white, preadipocytes (Supplementary Fig. 2). Importantly, expression of *Pgc-1α* and *Ucp1* was markedly induced by cAMP to 6- and 18-fold, respectively, in BMP7-treated cells (Fig. 1c), indicating that the differentiated lipid-containing cells induced by BMP7 are bona fide brown adipocytes with a complete capacity to initiate the thermogenic program. BMPs are known to stimulate osteogenic differentiation by inducing expression of the osteogenic runt related transcription factor 2 (RUNX2; ref. 11). In brown preadipocytes, BMP2, BMP6 and BMP7 significantly inhibited *Runx2* expression, whereas BMP4 had no effect (Fig. 1b), suggesting that these BMPs function in brown fat precursors to promote adipogenesis and inhibit osteogenic differentiation. The specific effect of BMP7 on brown preadipocyte differentiation was also verified in primary culture cells isolated from stromo-vascular fraction of interscapular BAT (Supplementary Fig 3).

Cellular responses to BMPs have been shown to be mediated by the formation of a hetero-oligomeric complex of the type 1 and type 2 BMP receptors (BMPRs). Two major signalling pathways, the SMAD (mothers against decapentaplegic *Drosophila* homologue) pathway and p38 MAP kinase pathway, confer most of the biological functions of BMPs[12]. We found there is only a subtle difference in expression levels of different BMPR isoforms between brown and white preadipocytes (Supplementary Fig. 4). Interestingly, whereas BMP7 increased phosphorylation of SMAD1/5/8 in both brown and white preadipocytes, robust activation of p38 MAP kinase and its downstream activating transcription factor (ATF)-2 after BMP7 stimulation was observed only in brown preadipocytes, while being blunted or almost completely absent in the 3T3-L1 white preadipocytes (Fig. 1d).

To investigate further the role of p38 MAP kinase in BMP7-induced brown adipogenesis, three pharmacological inhibitors of

[1]Section on Obesity and Hormone Action, and [2]Section on Cell and Molecular Physiology, Joslin Diabetes Center, Harvard Medical School, Boston, Massachusetts 02215, USA. [3]Division of Gastroenterology, Beth Israel Deaconess Medical Center, Harvard Medical School, Boston, Massachusetts 02215, USA. [4]Department of Biochemistry, Northwestern University, Evanston, Illinois 60208, USA. [5]Division of Pediatric Endocrinology, University of Iowa Children's Hospital, Iowa City, Iowa 52242, USA.

©2008 Macmillan Publishers Limited. All rights reserved

p38 MAP kinase were added individually to the medium 7 h before and throughout BMP7 treatment. After 10 days in culture, whereas none of these inhibitors had an effect on BMP7-induced lipid accumulation (Supplementary Fig. 5), all of these drugs effectively blocked the expression of UCP1 protein induced by BMP7 (Fig. 1e). p38 MAP kinase is known to regulate thermogenesis by means of nuclear coactivator PGC-1 (refs 13, 14). Indeed, we found that BMP7-induced UCP1 expression was markedly diminished in brown preadipocytes deficient in both PGC-1α and PGC-1β (ref. 15; Supplementary Fig. 6). Together, these data reveal an essential role for p38 MAP kinase and PGC-1 coactivators in the BMP7-induced thermogenic program in brown adipocytes, whereas they are dispensable for the effect of BMP7 on lipid accumulation.

Before entering the adipogenic program, preadipocytes must be released from suppressive factors and become committed to terminal differentiation[3]. Necdin acts as a negative modulator of brown preadipocyte differentiation, coordinating early adipogenic events, including suppression of preadipocyte factor-1 (PREF-1; also known as DLK1) and WNT10a expression[16]. Treatment of brown preadipocytes with BMP7 significantly suppressed expression of necdin (Fig. 2a). In addition, BMP7 also markedly suppressed gene expression of other inhibitors of adipogenesis, including PREF-1 and WNT10a (Fig. 2a). As a consequence of release from suppression by BMP7 treatment, these brown preadipocytes initiated the full transcriptional program of adipogenesis as shown by a significant increase in gene expression of PPARγ, C/EBPα and fatty acid binding protein 4 (FABP4, also known as aP2) (Fig. 2b). Importantly, BMP7 robustly induced expression of PRDM16, a zinc-finger binding protein recently identified as an early regulator determining brown fat fate[4], by 6.3-fold at day 3 (Fig. 2c). This led to increased expression of other molecular signatures of brown fat, including PGC-1α, PGC-1β (Fig. 2c) and UCP1 (Fig. 1b).

Differentiation of brown fat is accompanied by mitochondrial biogenesis[17]. In the brown preadipocyte cell line, BMP7 treatment significantly increased the expression of genes involved in mitochondrial biogenesis and function (Fig. 2c, d and Supplementary Fig. 1), including *Pgc-1α* and *Pgc-1β* as well as nuclear respiratory factor 1 (*Nrf1*), mitochondrial transcription factor A (*Tfam*) and cytochrome

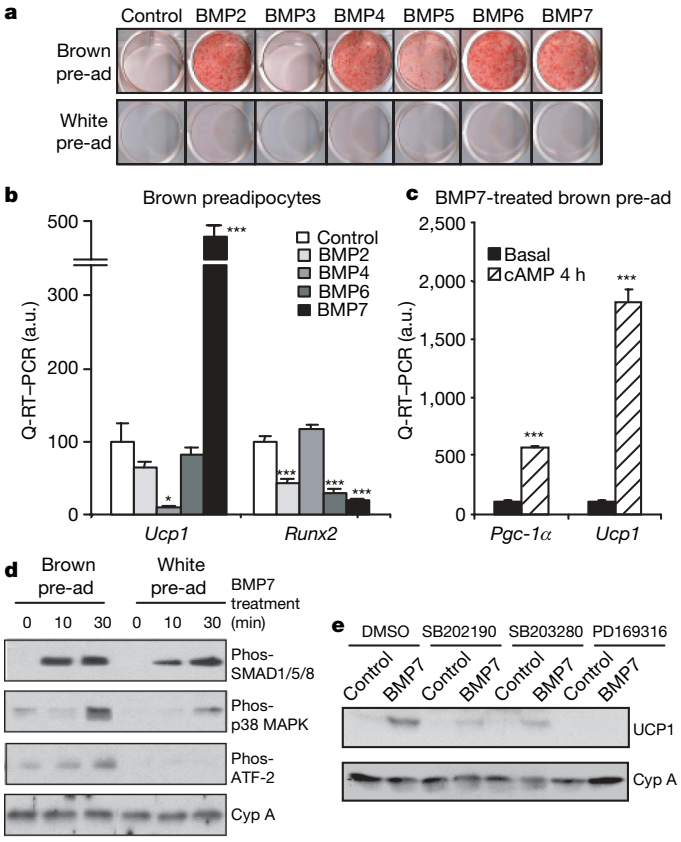

Figure 1 | BMP7 induces brown, but not white, preadipocyte differentiation, and the essential role of p38 MAPK in BMP7-induced thermogenesis. **a**, Oil Red O staining of brown preadipocytes and 3T3-L1 white preadipocytes (pre-ad) grown in growth medium supplemented with BMPs or vehicle (control) for 8 days. **b**, Quantitative reverse transcription polymerase chain reaction (Q-RT–PCR) analysis for *Ucp1* and *Runx2* in brown preadipocytes treated with vehicle or BMPs in a combination of insulin and T3 for 7 days. a.u., arbitrary units. **c**, Q-RT–PCR analysis for *Pgc-1α* and *Ucp1* in response to 4 h of cAMP stimulation in brown preadipocytes differentiated in growth medium supplemented with BMP7. Data are presented as mean ± s.e.m. ($n = 3$). Asterisks depict statistically significant differences between control and experimental groups ($^*P < 0.05$, $^{***}P < 0.001$). **d**, Western blot analysis of phosphorylation of SMAD1/5/8, p38 MAP kinase and ATF-2 in response to 0, 10 and 30 min of BMP7 stimulation in brown and white preadipocytes. Cyclophilin A (Cyp A) serves as a loading control. **e**, Western blot analysis of UCP1 in brown preadipocytes cultured in growth medium supplemented with vehicle or BMP7 for 10 days. Three p38 MAP kinase inhibitors or vehicle (DMSO) were added to the cells 7 h before and throughout BMP7 treatment.

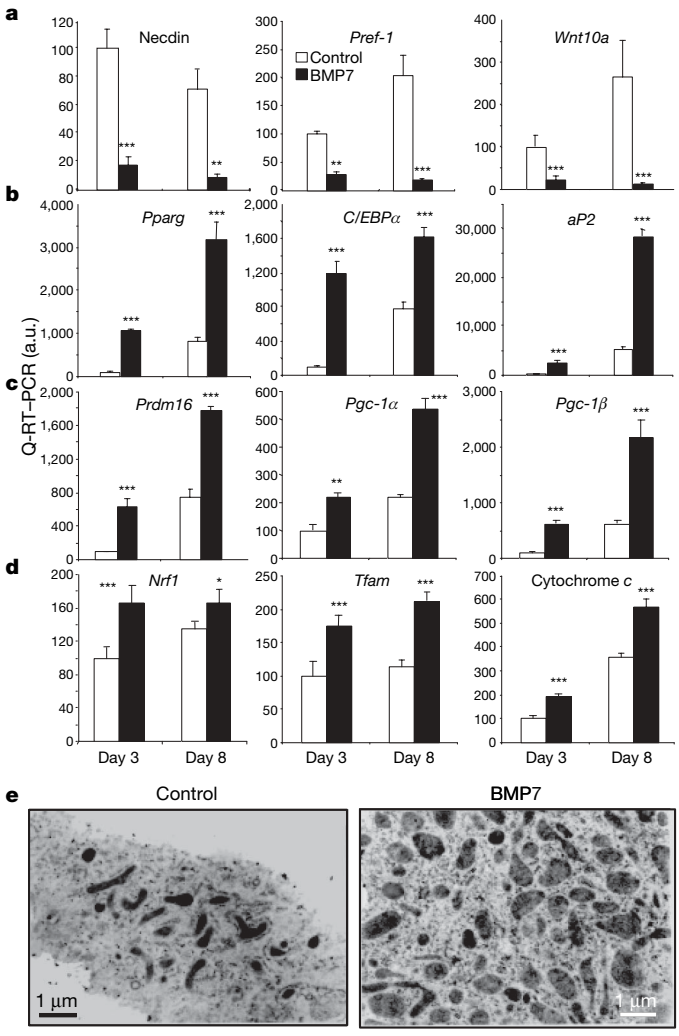

Figure 2 | Molecular mechanisms by which BMP7 induces brown adipogenesis and mitochondrial biogenesis. **a–d**, Q-RT–PCR analysis for genes encoding early adipogenic inhibitors (**a**), adipogenic markers common to brown and white fat (**b**), brown-fat-specific markers (**c**) and mitochondrial components (**d**) in brown preadipocytes treated with vehicle (control) or BMP7 for 3 or 8 days. Data are presented as mean ± s.e.m. ($n = 3$; $^*P < 0.05$, $^{**}P < 0.01$, $^{***}P < 0.001$). **e**, Transmission electron microscopy of brown preadipocytes treated with vehicle or BMP7 for 9 days. Original magnification, ×24,000.

©2008 Macmillan Publishers Limited. All rights reserved

c. This coincided with a fivefold increase in mitochondrial density in BMP7-treated cells compared to control (Fig. 2e). Thus, BMP7 activated a full program of brown adipogenesis by suppression of early adipogenic inhibitors, induction of factors determining brown fat fate, increased expression of adipogenic transcription factors and induction of mitochondrial biogenesis.

BMPs are important in the control of stem cell commitment to various lineages[18]. To determine whether BMP7 could also trigger commitment of the mesenchymal progenitor/stem cells into a brown adipocyte lineage, we treated the multipotent C3H10T1/2 cells with BMP7 for 3 days before treatment with a standard adipogenic differentiation cocktail[10]. Cells pretreated with BMP7, but not vehicle, displayed a mature brown adipocyte phenotype with marked increases in lipid accumulation, and induction of the brown-fat-specific protein UCP1 (Fig. 3a). Expression of specific markers indicated that the C3H10T1/2 cells had become committed to the brown adipocyte lineage within 3 days of BMP7 treatment (Fig. 3b). By this time point, BMP7 pre-treatment had increased expression of *C/EBPδ* (ref. 19), followed by increased expression of *C/EBPβ*, *C/EBPα*, *Pparg* and *aP2* at a later stage of differentiation, consistent with the previously described gene patterns in committed white and brown preadipocytes[20,21]. Interestingly, BMP7 pretreatment also caused a transient induction of *Pgc-1α* expression and a significant increase in expression of *Nrf1* and *Tfam*, followed by a later increase of cytochrome *c* expression (Fig. 3c), indicating increased mitochondrial biogenesis in these BMP7-pretreated cells during the course of brown adipogenesis.

To verify the cell culture findings *in vivo*, we implanted BMP7-treated C3H10T1/2 cells subcutaneously into athymic nude mice in the sternal region. Six weeks after implantation, the BMP7-treated cells developed into a fat pad containing a large number of multilocular and UCP1-positive brown adipocytes and a small portion of uni-locular white adipocytes, whereas no additional tissue was found in mice receiving cells treated with vehicle (Fig. 3d and Supplementary Fig. 7). Additionally, BMP7, in concert with other differentiating agents, induced brown adipogenesis in two more primitive fibroblastic cell lines with no adipogenic character (Supplementary Figs 8 and 9). Thus, BMP7 triggers commitment of multipotent mesenchymal cells to the brown adipocyte lineage in both *in vitro* and *ex vivo* settings.

To determine the physiological necessity of BMP7 for BAT development, we analysed brown fat morphology and function in *Bmp7* knockout mice. Because *Bmp7* null mice die shortly after birth[22,23], we focused our study in newborn mice and embryos. In rodents at these stages brown fat is already developed, whereas white fat is still not grossly visible. Notably, at birth, *Bmp7* knockout mice displayed a marked 50%–70% decrease in interscapular BAT mass compared with wild-type littermates, whereas the size of other internal organs, such as the liver, were not altered (Fig. 4a). The decrease of BAT mass in *Bmp7* knockout animals was also evident at embryonic stages. Cross-sections of 17.5 days postcoitum (d.p.c.) embryos showed a marked decrease in brown fat mass, associated with a marked decrease in the number of brown adipocytes (Fig. 4b and Supplementary Fig. 10). Most importantly, expression of UCP1 protein was markedly decreased or completely absent in brown fat from 18.5 d.p.c. *Bmp7* null embryos, whereas expression of insulin receptor, another protein involved in adipogenesis, remained unaltered (Fig. 4c). This was accompanied by a significant decrease in expression of a number of brown-fat-selective genes (Supplementary Fig. 11). These data establish an essential role of BMP7 in brown fat development *in vivo* and an almost absolute requirement for BMP7 in maintaining the brown-fat-specific thermogenic program.

Finally, to explore the potential role of BMP7 in regulation of brown adipogenesis and energy homeostasis *in vivo*, we injected adenoviruses expressing BMP3, BMP7 or LacZ (*Escherichia coli* β-galactosidase) as a control via the tail vein into 4-week-old C57BL/6 mice and measured metabolic rate by indirect calorimetry. Adenoviruses are trophic for the liver, where they can drive release of secretory proteins, such as BMPs, into the blood stream (Supplementary Fig. 12a). Importantly, mice that received adenovirus expressing BMP7 showed significant increases in whole-body energy expenditure and basal body temperature, leading to a significant reduction in weight gain compared with mice that received the LacZ adenovirus (Fig. 4d). The increase in energy expenditure in BMP7-treated mice was not due to an increase in physical activity or food intake (Supplementary Fig. 12). In contrast, BMP3, which had no effect on differentiation of brown preadipocytes *in vitro* (Fig. 1a), did not induce any metabolic effects compared to control mice. Fifteen days after adenoviral injection, mice that received BMP7 treatment displayed a significant

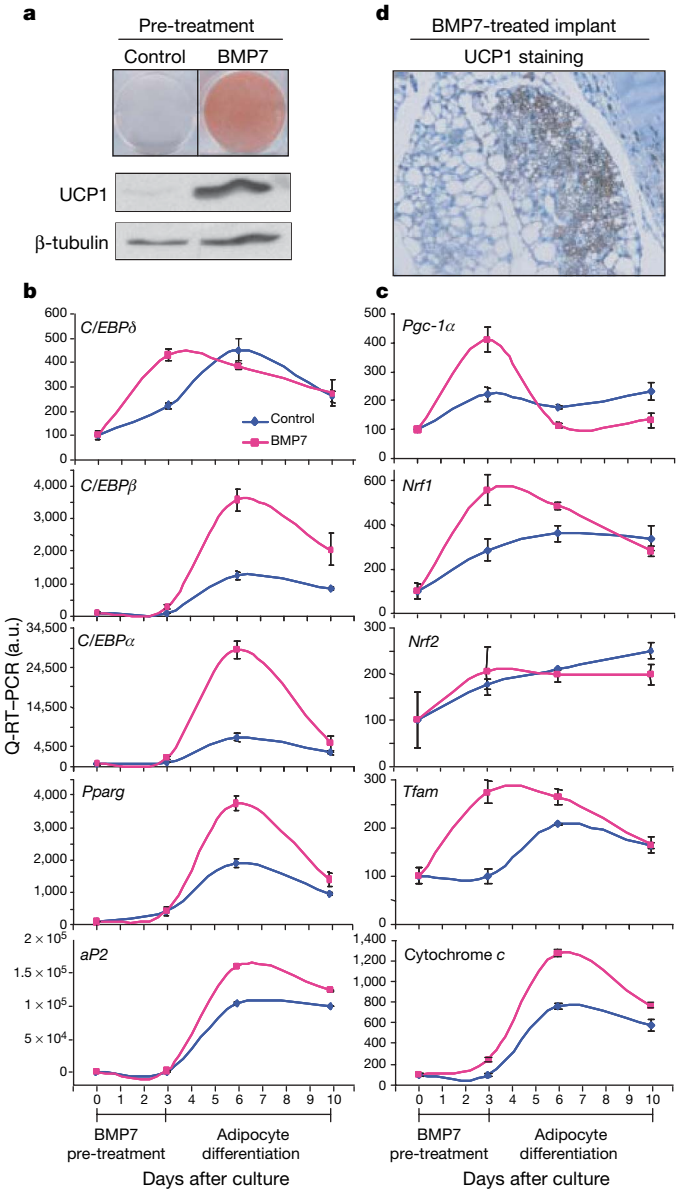

Figure 3 | BMP7 triggers commitment of mesenchymal progenitor cells to brown adipocyte lineage *in vitro* and *in vivo*. **a**, Oil Red O staining and western blotting analysis for UCP1 in C3H10T1/2 cells treated with BMP7 or vehicle (control) for 3 days followed by adipogenic induction for 7 days. β-tubulin serves as a loading control. **b**, **c**, Q-RT–PCR analysis for genes involved in the adipogenic program (**b**) and mitochondrial biogenesis (**c**) in cells described in **a**. Data are presented as mean ± s.e.m. ($n = 3$). **d**, UCP1 immunohistochemical staining on a tissue derived from implantation of BMP7-treated C3H10T1/2 cells into nude mice. Original magnification, ×400.

©2008 Macmillan Publishers Limited. All rights reserved

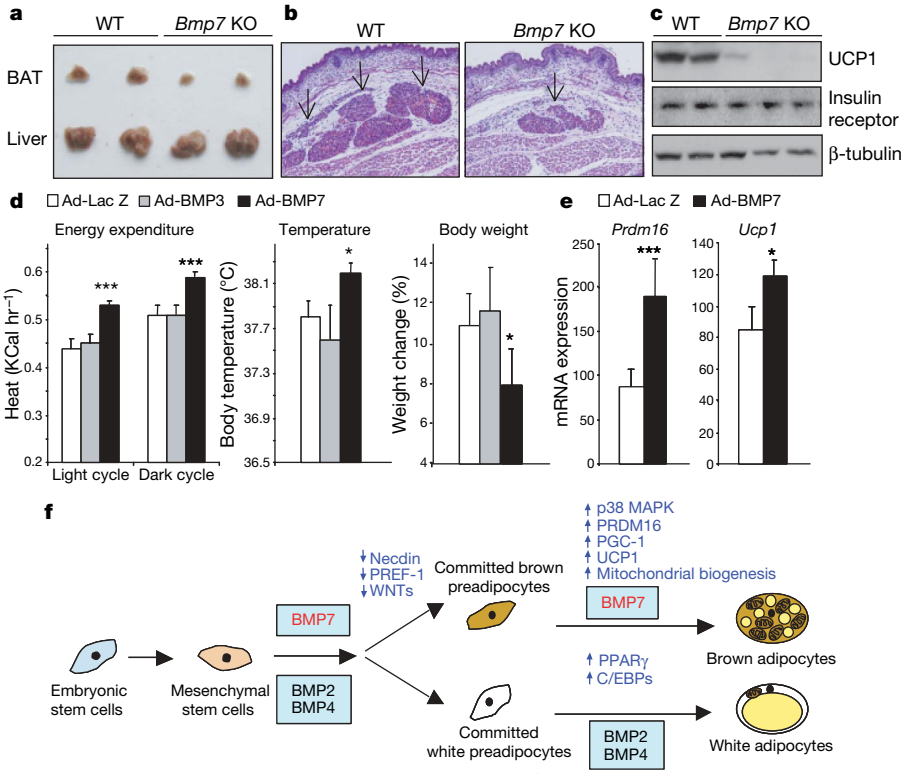

Figure 4 | Evidence for an essential role of BMP7 in BAT development, and regulation of whole-body energy expenditure by loss-of-function and gain-of-function approaches. **a**, Gross morphological analysis of BAT and liver from 1-day-old wild-type (WT) and *Bmp7* knockout (KO) pups. **b**, Transverse histological sections at the thoracic region from wild-type and *Bmp7* KO embryos at 17.5 d.p.c. Slides were stained by haematoxylin and eosin. Arrows indicate BAT. Original magnification is ×200. **c**, Western blotting analysis of UCP1 and insulin receptor β chain in BAT from wild-type and *Bmp7* KO embryos at 18.5 d.p.c. β-tubulin serves as a loading control. **d**, Adenoviruses (Ad) expressing BMP7, BMP3 or LacZ control were injected into 4-week-old C57BL/6 mice by means of the tail vein ($n = 5$). Energy expenditure was determined at 10 days after injection by indirect calorimetry. Basal body temperature was measured using a rectal thermometer after 14 days of injection. The significance of body weight change at day 5 after adenoviral injection was determined by Wilcoxon signed-rank test. **e**, Adenoviruses expressing BMP7 or LacZ control were injected into 12-week old C57BL/6 mice by means of the tail vein ($n = 6$). Mice were killed 15 days after injection. Expression of *Prdm16* and *Ucp1* in BAT was measured by Q-RT–PCR. Data are presented as mean ± s.e.m. Asterisks depict statistically significant differences between control and BMP7 groups ($^*P < 0.05$, $^{***}P < 0.001$). **f**, Proposed model for the role of BMPs in determination of brown versus white adipocyte development.

increase in brown fat mass with no change in WAT mass (Supplementary Fig. 13). In a cohort of older mice, BMP7 treatment specifically induced expression of *Prdm16* and *Ucp1* in BAT. They encode two key factors determining brown fat fate and function (Fig. 4e), whereas the expression of genes involved in energy homeostasis in other tissues, including WAT, muscle and liver, remained unaltered (Supplementary Fig. 14). Together, these data not only recapitulate the brown adipogenic effect of BMP7 *in vivo*, but also reveal an important anti-obesity potential of BMP7 by increasing whole-body thermogenesis.

BAT and WAT are morphologically and functionally different tissues, and their developmental patterns are quite distinct. One of the remaining questions in adipocyte biology is how and when the developmental fate of brown versus white adipocytes is regulated and specified. On the basis of the present data and published observations from other investigators[8,9,24], we propose a model for the role of BMPs in determination of brown versus white fat cell fate, as illustrated in Fig. 4f. Whereas BMP2 and BMP4 can promote differentiation of white adipocyte lineage, we demonstrate in the present study that BMP7 drives brown fat cell fate in both mesenchymal progenitor cells and committed brown preadipocytes. This is achieved by suppression of early adipogenic inhibitors, such as necdin, PREF-1 and WNTs, and by induction of key molecules that specify brown fat fate, such as PRDM16 and PGC-1α, leading to a mature brown adipocyte phenotype characterized by UCP1 expression and abundant mitochondria. *Bmp7* null embryos display brown fat hypoplasia and almost complete absence of UCP1 protein, highlighting an essential role of BMP7 in brown fat development. When used as a treatment *in vivo*, BMP7 is able to increase brown fat mass and thermogenic energy expenditure in mice.

Whereas BMP2, BMP4, BMP6 and BMP7 are able to induce massive lipid accumulation in brown preadipocytes, we find that only BMP7 has a specific effect on induction of the brown-fat-specific protein UCP1. Differential effects of various BMPs on other cell types have also been observed[25]. For example, BMP7, but not BMP4 or BMP6, is able to reverse the TGF-β-induced epithelial-to-mesenchymal transition in distal tubular epithelial cells[26]. Exactly how the specificity of different BMPs is determined remains an unsolved question in the field. Our data have indicated an important role of p38 MAP kinase and PGC-1 coactivator in BMP7-induced thermogenesis. Originally identified as a bone inducer[27], BMP7 is now being recognized as a multifunctional cytokine and has been implicated as a potential therapeutic agent for cardiovascular, metabolic and degenerative diseases[28]. In this study, our data reveal a novel function of BMP7 in the regulation of energy homeostasis by promoting brown, but not white, fat differentiation and function. Thus, we propose that treatment of humans with BMP7 or its molecular mimetic may activate brown fat differentiation, leading to an increase in energy expenditure, and thereby providing a new way to combat obesity.

METHODS SUMMARY

Adipocyte differentiation. To induce adipocyte differentiation by BMPs in the absence of induction cocktails, both wild-type brown preadipocytes and 3T3-L1

©2008 Macmillan Publishers Limited. All rights reserved

white preadipocytes were grown in regular growth medium supplemented with a combination of recombinant human BMPs (rhBMPs, 3.3–8.3 nM), insulin (20 nM) and triiodothyronine (T3, 1 nM) or vehicle as indicated in the text and figure legends for 7–13 days. To stimulate the thermogenic program, differentiated cells were incubated with 500 μM dibutyrul cAMP for 4 h. Cells were grown in growth medium without hormonal supplements for 18 h before cAMP stimulation.

C3H10T1/2 cells were grown in the presence and absence of 8.3 nM rhBMP7 for 3 days to reach confluence (day 3). These cells were then induced to adipocyte differentiation using protocols described below for an additional 7 days (day 10). Adipocyte differentiation was performed by treating confluent cells for 48 h in medium supplemented with 20 nM insulin and 1 nM T3, 0.5 μM isobutylmethylxanthine (IBMX), 5 mM dexamethasone, and 0.125 mM indomethacin. Cells were placed back in growth medium supplemented with insulin and T3, which was then changed every second day. After four to five more days in this medium, cells exhibited a fully differentiated phenotype with massive lipid accumulation.

Full Methods and any associated references are available in the online version of the paper at www.nature.com/nature.

Received 27 February; accepted 27 June 2008.

1. Gesta, S., Tseng, Y. H. & Kahn, C. R. Developmental origin of fat: tracking obesity to its source. *Cell* **131,** 242–256 (2007).
2. Farmer, S. R. Transcriptional control of adipocyte formation. *Cell Metab.* **4,** 263–273 (2006).
3. Rosen, E. D. & MacDougald, O. A. Adipocyte differentiation from the inside out. *Nature Rev. Mol. Cell Biol.* **7,** 885–896 (2006).
4. Seale, P. *et al.* Transcriptional control of brown fat determination by PRDM16. *Cell Metab.* **6,** 38–54 (2007).
5. Puigserver, P. *et al.* A cold-inducible coactivator of nuclear receptors linked to adaptive thermogenesis. *Cell* **92,** 829–839 (1998).
6. Chen, D., Zhao, M. & Mundy, G. R. Bone morphogenetic proteins. *Growth Factors* **22,** 233–241 (2004).
7. Tseng, Y. H. & He, T. C. Bone morphogenetic proteins and adipocyte differentiation. *Cellscience Rev.* **3,** 342–360 (2007).
8. Wang, E. A., Israel, D. I., Kelly, S. & Luxenberg, D. P. Bone morphogenetic protein-2 causes commitment and differentiation in C3H10T1/2 and 3T3 cells. *Growth Factors* **9,** 57–71 (1993).
9. Tang, Q. Q., Otto, T. C. & Lane, M. D. Commitment of C3H10T1/2 pluripotent stem cells to the adipocyte lineage. *Proc. Natl Acad. Sci. USA* **101,** 9607–9611 (2004).
10. Klein, J. *et al.* β_3-adrenergic stimulation differentially inhibits insulin signaling and decreases insulin induced glucose uptake in brown adipocytes. *J. Biol. Chem.* **274,** 34795–34802 (1999).
11. Ducy, P., Zhang, R., Geoffroy, V., Ridall, A. L. & Karsenty, G. Osf2/Cbfa1: a transcriptional activator of osteoblast differentiation. *Cell* **89,** 747–754 (1997).
12. Canalis, E., Economides, A. N. & Gazzerro, E. Bone morphogenetic proteins, their antagonists, and the skeleton. *Endocr. Rev.* **24,** 218–235 (2003).
13. Puigserver, P. *et al.* Cytokine stimulation of energy expenditure through p38 MAP kinase activation of PPARγ coactivator-1. *Mol. Cell* **8,** 971–982 (2001).
14. Cao, W. *et al.* p38 mitogen-activated protein kinase is the central regulator of cyclic AMP-dependent transcription of the brown fat uncoupling protein 1 gene. *Mol. Cell. Biol.* **24,** 3057–3067 (2004).
15. Uldry, M. *et al.* Complementary action of the PGC-1 coactivators in mitochondrial biogenesis and brown fat differentiation. *Cell Metab.* **3,** 333–341 (2006).
16. Tseng, Y. H. *et al.* Prediction of preadipocyte differentiation by gene expression reveals role of insulin receptor substrates and necdin. *Nature Cell Biol.* **7,** 601–611 (2005).
17. Nedergaard, J., Connally, E. & Cannon, B. *Brown Adipose Tissue* (eds Trayhurn, P. & Nicholls, D. G.) 152–213 (Arnold, 1986).
18. Varga, A. C. & Wrana, J. L. The disparate role of BMP in stem cell biology. *Oncogene* **24,** 5713–5721 (2005).
19. Darlington, G. J., Ross, S. E. & MacDougald, O. A. The role of C/EBP genes in adipocyte differentiation. *J. Biol. Chem.* **273,** 30057–30060 (1998).
20. Wu, Z. *et al.* Cross-regulation of C/EBPαand PPARγ controls the transcriptional pathway of adipogenesis and insulin sensitivity. *Mol. Cell* **3,** 151–158 (1999).
21. Tseng, Y. H., Kriauciunas, K. M., Kokkotou, E. & Kahn, C. R. Differential roles of insulin receptor substrates in brown adipocyte differentiation. *Mol. Cell. Biol.* **24,** 1918–1929 (2004).
22. Dudley, A. T., Lyons, K. M. & Robertson, E. J. A requirement for bone morphogenetic protein-7 during development of the mammalian kidney and eye. *Genes Dev.* **9,** 2795–2807 (1995).
23. Luo, G. *et al.* BMP-7 is an inducer of nephrogenesis, and is also required for eye development and skeletal patterning. *Genes Dev.* **9,** 2808–2820 (1995).
24. Jin, W. *et al.* Schnurri-2 controls BMP-dependent adipogenesis via interaction with Smad proteins. *Dev. Cell* **10,** 461–471 (2006).
25. Cheng, H. *et al.* Osteogenic activity of the fourteen types of human bone morphogenetic proteins (BMPs). *J. Bone Joint Surg. Am.* **85-A,** 1544–1552 (2003).
26. Zeisberg, M. *et al.* BMP-7 counteracts TGF-β1-induced epithelial-to-mesenchymal transition and reverses chronic renal injury. *Nature Med.* **9,** 964–968 (2003).
27. Ozkaynak, E. *et al.* OP-1 cDNA encodes an osteogenic protein in the TGF-β family. *EMBO J.* **9,** 2085–2093 (1990).
28. Tobin, J. F. & Celeste, A. J. Bone morphogenetic proteins and growth differentiation factors as drug targets in cardiovascular and metabolic disease. *Drug Discov. Today* **11,** 405–411 (2006).

Supplementary Information is linked to the online version of the paper at www.nature.com/nature.

Acknowledgements We acknowledge T.-C. He for providing adenoviruses expressing BMPs. We thank M. Rourk and L. Mazzola for help with the animal experiments, J. Hu, C. Cahill, A. McSweeney, L. Polivy and R. Bronson for technical assistance, and P. Zhang for statistical consultation. We thank A. Butte and P. Laustsen for inputs on initiation of this project. We thank M. Uldry and B. Spiegelman for providing the PGC-1 null cells. This work was supported in part by the National Institutes of Health grants R01 DK077097, R21 DK070722, P30 DK46200 and P30 DK040561 (to Y.-H.T.), R01 DK67536 (to R.N.K.), K08 DK64906 (to A.W.N.) and R01 DK 060837 (to C.R.K), the Tanita Healthy Weight Community, and the Eleanor and Miles Shore 50th Anniversary Scholar Program from Harvard Medical School (to Y.-H.T.).

Author Information Reprints and permissions information is available at www.nature.com/reprints. Correspondence and requests for materials should be addressed to Y.-H.T. (yu-hua.tseng@joslin.harvard.edu).

©2008 Macmillan Publishers Limited. All rights reserved

METHODS

Materials. Recombinant human BMPs were purchased from R&D Systems. Antibodies used for immunoblotting included anti-UCP1, anti-PPARγ, anti-β-tubulin (all purchased from Santa Cruz Biotechnology), anti-FAS (a gift from F. P. Kuhajda), anti-phospho-SMAD1/5/8, anti-phospho-p38 MAPK, anti-phospho-ATF-2, anti-β-tubulin, anti-insulin receptor β subunit (Cell Signaling) and anti-cyclophilin A (Upstate Biotechnology). Immobolin-P transfer membranes were from Millipore and electrophoresis supplies were from Bio-Rad Laboratories. SB202190, SB203280 and PD169316 were purchased from Calbiochem and dissolved in DMSO. All other chemicals were purchased from Sigma Chemical Co. unless otherwise specified.

Cell culture. C3H10T1/2 and 3T3-L1 cells were purchased from American Type Culture Collection. Generation of wild-type brown preadipocyte cell lines derived from newborn wild-type mice was as described previously[10,29–31]. The PGC-1 null brown preadipocyte cell line was a gift from B. M. Spiegelman[15]. All cell lines used in this study were maintained in Dulbecco's modified Earle's medium (DMEM) 10% fetal clone III (HyClone) at 37 °C in 5% CO_2 environment unless otherwise specified.

Q-RT–PCR analysis. Total RNA was isolated with QIAzol lysis reagent (Qiagen) and purified by RNeasy Mini columns (Qiagen) following the manufacturer's instructions. Complementary DNA was prepared from 1 μg of RNA using the Advantage RT–PCR kit (BD Biosciences) according to the manufacturer's instructions and diluted to a final volume of 250 μl. Five microlitres of diluted cDNA was used in a 20 μl PCR reaction with SYBR Green Master Mix (Applied Biosystems) and primers at a concentration of 300 nM each. PCR reactions were run in duplicate for each sample and quantified in the ABI Prism 7000 Sequence Detection System (Applied Biosystems). Data were expressed as arbitrary units after normalization to levels of expression of the internal control acidic ribosomal phosphoprotein P0 (Arbp, 36B4) for each sample. Sequences of primers used in this study are listed in Supplementary Table 2.

Oil red O staining. Dishes were washed twice with phosphate-buffered saline and fixed with 10% buffered formalin for 16 h at 4 °C. Cells were then stained for 2 h at room temperature with a filtered Oil red O solution (0.5% Oil red O in isopropyl alcohol), washed twice with distilled water, and visualized.

Western blot analysis. Cells were collected in lysis buffer (50 mM HEPES, 137 mM NaCl, 1 mM $MgCl_2$, 1 mM $CaCl_2$, 10 mM $Na_2P_2O_7$, 10 mM NaF, 2 mM EDTA, 10% glycerol, 1% Igepal CA-630, 2 mM vanadate, 10 μg ml^{-1} leupeptin, 10 μg ml^{-1} aprotinin and 2 mM phenylmethylsulfonyl fluoride, pH 7.4). After lysis, lysates were clarified by centrifugation at 12,000*g* for 20 min at 4 °C; the protein amount in the supernatants was determined by the Bradford Protein Assay (Bio-Rad Laboratories). Proteins were directly solubilized in Laemmli sample buffer. Equal amounts of proteins were separated by SDS-polyacrylamide gel electrophoresis and transferred to Immobolin-P membranes. Membranes were blocked overnight at 4 °C and incubated with the indicated antibody for 2 h at room temperature. Specifically bound primary antibodies were detected with peroxidase-coupled secondary antibody and enhanced chemiluminescence (Amersham Biosciences).

Electron microscopy. Cells were fixed in 2.5% glutaraldehyde, and then post-fixed in 2% osmium teroxide, dehydrated in ascending gradations of ethanol, and embedded in fresh Araldite 502 epoxy resin using BEEM capsules. Ultra-thin sections (60–80 nm) were cut and mounted on 75 mesh copper grids, and then stained with uranyl acetate and lead citrate before being examined on the Phillips 301 transmission electron microscope. Mitochondrial and total cytoplasmic areas were quantified by using the NIH Image J software (http://rsb.info.nih.gov/ij/). Mitochondrial density was determined by the ratio of the sum of mitochondrial area to total cytoplasmic area per cell.

Isolation of stromo-vascular fractions and *in vitro* differentiation. Eight 6-week-old C57BL/6 male mice were killed. Interscapular BAT and axillary subcutaneous WAT were removed, minced and digested with 1 mg ml^{-1} collagenase for 45 min at 37 °C in DMEM/F12 medium containing 1% BSA and antibiotics. Digested tissues were filtered through sterile 150 μm nylon mesh and centrifuged at 250*g* for 5 min. The floating fractions consisting of adipocytes were discarded and the pellets representing the stromo-vascular fractions were then resuspended in erythrocyte lysis buffer (154 mM NH_4Cl, 10 mM $KHCO_3$, 0.1 mM EDTA) for 10 min to remove red blood cells. The cells were further centrifuged at 500*g* for 5 min, plated at 8×10^5 per well of a 24-well plate and grown at 37 °C in DMEM/F12 supplemented with 10% FBS at 37 °C.

In vitro differentiation was performed using the method described in ref. 32. After 2 days of incubation, the attached cells were washed and incubated in serum-free differentiation medium containing DMEM/F12 medium supplemented with 1 μM dexamethasone, 66 nM insulin, 15 mM HEPES, 1 nM T3, 33 μM biotin, 17 μM pantothenate, 10 μg ml^{-1} transferrin and 100 μg ml^{-1} penicillin-streptomycin in the absence or presence of 1 μg ml^{-1} rosiglitazone or 3.3 nM rhBMP7 for 3 days.

Implantation. C3H10T1/2 cells were grown in the presence and absence of 3.3 nM rhBMP7 for 3 days to reach confluence. Cells were washed, trypsinized, and resuspended in growth medium. 1.5×10^7 cells in 0.15 ml volume were injected into the thoracic/sternum region of 5-week-old BALB/c athymic mice (Charles River Laboratories, Inc.) using an 18-gauge needle. Mice were killed 6 weeks after injection, and adipose tissue derived from implanted cells was excised and processed for histological analysis.

Histology and immunohistochemistry. Tissues were fixed in 10% formalin and were paraffin-embedded. Multiple sections were prepared and stained with haematoxylin and eosin for general morphological observation. UCP1 immunohistochemistry of tissue from implanted cells was performed using polyclonal anti-mouse UCP1 antibody (Chemicon International Inc.) at 1:50 dilution and the Dako Envision Doublestain System (Dako) following the manufacturer's instruction. Slides were counterstained with haematoxylin.

Genotyping of *Bmp7* null mice. *Bmp7* null mice were produced by intercrosses of animals heterozygous for a null allele of *Bmp7* generated by an insertion of *lacZ* into exon 1 (ref. 33). Genotypes were initially determined by a combination of β-galactosidase staining and the presence or absence of a severe eye phenotype (very small eyes or no eye)[22,23,33]. All genotypes were confirmed by PCR as described in ref. 34. For β-galactosidase staining, the tips of tails were clipped, and fixed in 4% PFA plus 2 mM $MgCl_2$ in PBS for 30 min at room temperature. The tails were washed in 2 mM $MgCl_2$ in PBS 3 times for 10 min at room temperature. The tails were stained at 37 °C overnight in X-gal staining solution (5 mM potassium ferrocyanide, 5 mM potassium ferricyanide, 2 mM $MgCl_2$ and 0.5 mg ml^{-1} 5-bromo-4-chloro-3-indolyl-β-D-galactosidase X-gal, Denville Scientific, Inc.). The presence of β-galactosidase staining in the tails indicates that the *lacZ* transgene is present in *Bmp7* exon 1. A lack of β-galactosidase staining indicates the mouse is wild type.

Adenoviral injection. Adenoviruses were amplified in HEK293 cells as described previously[35]. Before *in vivo* use, all adenoviruses were purified on a caesium chloride gradient and dialysed into PBS plus 10% glycerol. Four- and twelve-week-old male C57BL/6 mice were injected via the tail vein with an adenoviral dose of 5×10^8 viral particles per g body weight as described previously[36]. Mice were killed 15 days after injection. Interscapular brown fat and epididymal white fat were excised and weighted. Half of the tissue was fixed in 10% formalin and processed for histological analysis. The other half of the tissue was subjected to RNA extraction and Q-RT–PCR analysis.

Indirect calorimetry. Metabolic rates were measured by indirect calorimetry in mice 7–10 days after adenoviral injection by using the Comprehensive Lab Animal Monitoring System (CLAMS, Columbus Instruments). Mice were maintained at 24 °C under a 12-h light/dark cycle. Food and water were available *ad libitum*. Mice were acclimatized to individual cages for 24 h before recording, and then underwent 24 h of monitoring.

Heat production (energy expenditure) was calculated using the following equation:

$$\text{Heat} = [3.815 + 1.232(V_{CO2}/V_{O2})] \times V_{O2} \times \text{body weight}$$

where heat is measured in kcal h^{-1}, V_{O2} is measured in litres kg^{-1} h^{-1} and body weight is measured in kg.

Measurement of plasma BMP7 concentrations. Blood was collected at day 1 and day 3 after adenoviral injection and at the time the mouse was killed. Plasma BMP7 levels were determined by ELISA using the DuoSet ELISA Development kit purchased from R&D Systems following the manufacturer's instructions. Concentrations were calculated using a standard curve generated by rhBMP7 standards included in the kit.

Statistical analysis. Statistical significance in gene expression between the control and the BMP-treated group was determined by analysis of variance (ANOVA) test or Student's *t* test unless otherwise specified. To evaluate if there was a significant change in body weight between BMP7 and control groups, we performed a multivariate ANOVA (MANOVA) test. Based on multivariate normal assumption on the data, Hotelling's T^2 statistics was calculated and yielded $T^2 = 3.9613$ and a significant *P*-value of 0.0191. The T^2 test of Harold Hotelling compares means of two or more continuous measures simultaneously for the two groups. Considering the small size of samples and the validity of multivariate normal assumption, we also performed the sign- and rank-based MANOVA analyses. The sign-based MANOVA gave a *P*-value of 0.0581 and the rank-based MANOVA yielded a *P*-value of 0.0612. Both are marginally statistically significant. Comparison was also conducted at different time points individually. We found that at day 5 after adenoviral injection, the percentage of body weight changes relative to the initial body weight was significant between the control and the BMP7 groups (*P*-value = 0.0469 by Wilcoxon signed-rank test).

29. Fasshauer, M. *et al.* Essential role of insulin receptor substrate-2 in insulin stimulation of glut4 translocation and glucose uptake in brown adipocytes. *J. Biol. Chem.* **275**, 25494–25501 (2000).

©2008 Macmillan Publishers Limited. All rights reserved

30. Fasshauer, M. *et al.* Essential role of insulin receptor substrate 1 in differentiation of brown adipocytes. *Mol. Cell. Biol.* **21,** 319–329 (2001).
31. Tseng, Y. H., Ueki, K., Kriauciunas, K. M. & Kahn, C. R. Differential roles of insulin receptor substrates in the anti-apoptotic function of insulin-like growth factor-1 and insulin. *J. Biol. Chem.* **277,** 31601–31611 (2002).
32. Hauner, H. *et al.* Promoting effect of glucocorticoids on the differentiation of human adipocyte precursor cells cultured in a chemically defined medium. *J. Clin. Invest.* **84,** 1663–1670 (1989).
33. Godin, R. E., Takaesu, N. T., Robertson, E. J. & Dudley, A. T. Regulation of BMP7 expression during kidney development. *Development* **125,** 3473–3482 (1998).
34. Bandyopadhyay, A. *et al.* Genetic analysis of the roles of BMP2, BMP4, and BMP7 in limb patterning and skeletogenesis. *PLoS Genet.* **2,** e216 (2006).
35. Ueki, K., Kondo, T., Tseng, Y. H. & Kahn, C. R. Central role of suppressors of cytokine signaling proteins in hepatic steatosis, insulin resistance, and the metabolic syndrome in the mouse. *Proc. Natl Acad. Sci. USA* **101,** 10422–10427 (2004).
36. Laustsen, P. G. *et al.* Lipoatrophic diabetes in *Irs1*$^{-/-}$/*Irs3*$^{-/-}$ double knockout mice. *Genes Dev.* **16,** 3213–3222 (2002).

©2008 Macmillan Publishers Limited. All rights reserved

CORRIGENDUM

doi:10.1038/nature08038

New role of bone morphogenetic protein 7 in brown adipogenesis and energy expenditure

Yu-Hua Tseng, Efi Kokkotou, Tim J. Schulz, Tian Lian Huang, Jonathon N. Winnay, Cullen M. Taniguchi, Thien T. Tran, Ryo Suzuki, Daniel O. Espinoza, Yuji Yamamoto, Molly J. Ahrens, Andrew T. Dudley, Andrew W. Norris, Rohit N. Kulkarni & C. Ronald Kahn

Nature **454**, 1000–1004 (2008)

In the Methods Summary of this Letter, the concentrations of IBMX and dexamethasone were incorrectly listed as 0.5 μM and 5 mM, respectively. The correct concentrations are 0.5 mM IBMX and 5 μM dexamethasone.

©2009 Macmillan Publishers Limited. All rights reserved